

# Vision and UWB-Based Anchor Self-Localisation System for UAV in GPS-Denied Environment

Beiya Yang, Erfu Yang\* and Leijian Yu

Department of Design, Manufacturing and Engineering Management, University of Strathclyde, 75 Montrose Street, Glasgow G1 1XJ, UK

\*erfu.yang@strath.ac.uk

**Abstract.** With the increasing applications of unmanned aerial vehicles (UAVs) in industries, it has drawn dramatic interests that utilising UAVs for internal inspection of oil tanks and vessels in recent years. Due to the fact that there is no global positioning system (GPS) and limited prior knowledge about operational environment, it is an unsolved problem on how to get the precise position information without relying on prior knowledge. To solve this problem, a Vision Aided Self-Localisation Two-way Time of Flight (VASTWTOF) algorithm is proposed. In the proposed algorithm, ultra-wideband (UWB) based sensor nodes are utilised for UAVs to achieve precise localisation in GPS-denied environment and the vision-based approach is adopted for anchor self-localisation. The simulation results show that the proposed algorithm can greatly improve the localisation performance and could be used for UAVs' precise localisation in GPS-denied environment, especially for the internal inspection of oil tanks and vessels.

## 1. Introduction

Unmanned aerial vehicles (UAVs) can be deployed into confined areas such as oil tanks and vessels where they are normally unsafe and hard for humans to access [1]. Therefore, utilising UAVs for inner inspection is growing dramatically [2]. However, unlike the outdoor environment, global positioning system (GPS) is unavailable inside oil tanks and vessels. As a result, achieving the precise localisation for UAVs to keep stable in GPS-denied environment is one key requirement to perform inspection tasks. Currently, the precise indoor positioning technologies can be divided into three types, i.e.: wave propagation, vision-based and inertial navigation technologies [3]. Wave propagation technologies utilise propagation properties of the radio or sound for localisation. Vision-based indoor positioning approaches are based on image or video processing technologies for positioning. Inertial navigation technologies leverage inertial measurement unit (IMU) to realise the positioning system. Among these technologies, ultra-wideband (UWB) based localisation technology is the most reliable, robust and low-cost approach which is suitable for our application [4]. Nowadays, lots of researchers have already made great attempts in developing the UWB-based high accuracy indoor localisation systems. In the existing work, it is always assumed that UWB anchor nodes are fixed and their relative positions are known [5]. However, in GPS-denied environment such as oil tanks or vessels, the position information of anchor nodes often needs to be manually measured by the engineers who place the nodes in operation. As a result, this would influence the localisation performance greatly. On the other hand, the vision-based localisation approach has had a great success to locate objects in many areas [6]. Thus, it is desirable and advantageous to develop an alternative approach to solve the existing issue with the adoption of vision-based techniques.



Toward this end, a Vision Aided Self-Localisation Two-Way Time of Flight (VASTWTOF) algorithm is proposed in this paper to provide the accurate and flexible indoor localisation function for UAVs in GPS-denied environment.

## 2. Vision-based Anchor Self-localisation Algorithm

To get the precise position information of UAV in GPS-denied environment, a fixed camera is utilised to measure the relative position of the visual markers (anchor nodes) first. Then, a coordinate frame is able to be constructed according to the calculated anchor positions. Finally, the position information of UAV can be estimated through the calculated position information of anchor nodes and time of flight (TOF) information measured by the UWB sensor nodes. Considering the z-coordinate could be measured by the existing barometer or IMU on flight controller of UAV directly, here we only considered the localisation for one UAV in 2D scene. The flowchart of the system is given in Figure 1.

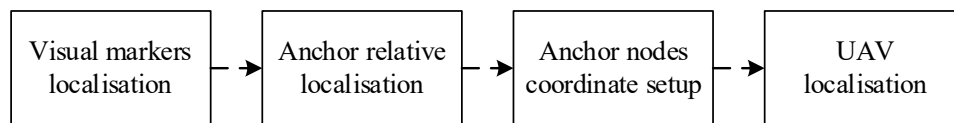


Figure 1. System flowchart

In this study, the Aruco markers [7] are adopted to realise the anchor self-localisation. In general, Aruco markers are the squares containing a black border and an inner grid that is used to store a specific binary code for identification. The marker detection technology is based on the OpenCV library [8]. The adaptive thresholding technology is applied to the image first. Then, the contours are detected through a contour extractor with filters. The potential corners of the marker were transferred by the perspective transformation operations. With the help of the Otsu method [9], the marker can be represented by binary values. After that, the marker is divided into small cells, and the inner code of the marker will be analysed to check whether it belongs to a specific tag dictionary. As the four corners  $(x_1, y_1, x_2, y_2, x_3, y_3, x_4, y_4)$  in a counter-clockwise manner) of the marker in the image and the real size  $(S_m, S_m)$  of the marker are known, the real distance of one pixel represented in real world  $S_{pr}$  can be calculated. To get a more accurate result, the mean value is adopted:

$$S_{pr} = 4S_m / (|x_1 - x_4| + |x_2 - x_3| + |y_1 - y_2| + |y_4 - y_3|) \quad (1)$$

## 3. Two-way Time of Flight (TW-TOF) Localisation Algorithm

Thanks to the precise anchor position information estimated through the vision-based approach, the signal propagation delay between anchor nodes and UAV is exploited to estimate the position information of UAV by utilising the TW-TOF localisation algorithm [10]. The localisation model for the algorithm is shown in Figure 2.

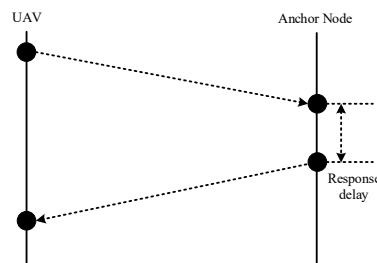


Figure 2. Localisation model for TW-TOF

According to Figure 2, the propagation delay between the anchor node and UAV can be represented as:

$$d_{UA} = [(t_{U2} - t_{U1}) - (t_{A2} - t_{A1})] / 2 \quad (2)$$

Where  $d_{UA}$  is the time delay between the anchor node and UAV,  $t_{U1}$ ,  $t_{U2}$  denote the measured time of departure (TOD) and time of arrival (TOA) for UAV,  $t_{A1}$ ,  $t_{A2}$  represent the measured TOA and TOD for the anchor node. Suppose the measured TOD and TOA to be denoted as:

$$\varphi(t) = \tilde{\varphi}(t) + n(t), \quad l(t) = \tilde{l}(t) + n(t) \quad (3)$$

Where  $\tilde{\varphi}(t)$  and  $\tilde{l}(t)$  are the true value of TOD and TOA, respectively.  $n(t)$  is an additive white Gaussian noise with a zero mean and  $\sigma_n^2$  variance,  $n(t) \square N(0, \sigma_n^2)$ . So, the propagation delay between anchor and UAV can be represented as:

$$z(t) = \left[ (l_U(t) - \varphi_U(t)) - (\varphi_A(t) - l_A(t)) \right] / 2 \quad (4)$$

Thus, we can get  $N$  measurement equations from anchor nodes which can be written into a matrix form:

$$\mathbf{z} = f(\mathbf{x}_U) + \mathbf{w} \quad (5)$$

Where,  $\mathbf{x}_U$  is the x-y coordinate of UAV, can be denoted as  $\mathbf{x}_U = [x_U, y_U]^T$ . In which  $d_N$  is the time delay between UAV and anchor  $N$ ,  $c$  is the speed of light and  $\mathbf{w}$  is the measurement noise. Therefore, the likelihood function can be written as:

$$p(\mathbf{z} | \mathbf{x}_U) = \frac{1}{(2\pi)^{\frac{N}{2}} \det(\mathbf{Q}_w)^{\frac{1}{2}}} \cdot \exp \left[ -\frac{1}{2} (\mathbf{z} - f(\mathbf{x}_U))^T \mathbf{Q}_w^{-1} (\mathbf{z} - f(\mathbf{x}_U)) \right] \quad (6)$$

Where  $\mathbf{Q}_w$  represents the covariance matrix of  $\mathbf{w}$ . From equation (6), it can be found that:

$$\hat{\mathbf{x}}_U = \arg \min \left[ (\mathbf{z} - f(\mathbf{x}_U))^T \mathbf{Q}_w^{-1} (\mathbf{z} - f(\mathbf{x}_U)) \right] \quad (7)$$

However, due to the nonlinearity of  $f(\mathbf{x}_U)$ , a closed-form solution to equation (7) does not exist. So, the numerical minimization technique is required to solve this. Here, let the estimation of  $\hat{\mathbf{x}}_U$  at  $k$  th iteration be  $\hat{\mathbf{x}}_U(k)$  and  $\hat{\mathbf{x}}_U(k+1) = \hat{\mathbf{x}}_U(k) + \Delta(k)$ . Linearising  $f(\mathbf{x}_U)$  around  $\hat{\mathbf{x}}_U(k)$  yields:

$$f(\mathbf{x}_U) \approx f(\hat{\mathbf{x}}_U(k)) + G(\hat{\mathbf{x}}_U(k)) \Delta(k) \quad (8)$$

Where  $G(\hat{\mathbf{x}}_U(k))$  represents the Jacobian matrix of  $f(\mathbf{x}_U)$ . Thus,  $\Delta(k)$  can be written as:

$$\Delta(k) = \left[ G^T(\hat{\mathbf{x}}_U(k)) \mathbf{Q}_w^{-1} G(\hat{\mathbf{x}}_U(k)) \right]^{-1} \cdot G^T(\hat{\mathbf{x}}_U(k)) \mathbf{Q}_w^{-1} \left[ \mathbf{z} - f(\hat{\mathbf{x}}_U(k)) \right] \quad (9)$$

Therefore, the estimation of  $\hat{\mathbf{x}}_U(k)$  at  $k$  th iteration can be calculated finally. For the start of the iteration, an initial value for UAV is needed. The estimated position from the last localisation period can be used as the initial value to reduce the number of iterations.

#### 4. System Simulation and Discussion

In order to verify the proposed VASTWTOF algorithm, the following simulations are carried out. A 2D scene ( $10m \times 10m$ ) with four anchor nodes is considered in this paper. The localisation model is shown following Figure 3, where four markers are placed under each anchor nodes. The hybrid V-REP and MATLAB simulation platform are utilised to simulate the VASTWTOF and localisation system shown in Figure 4(a). Furthermore, in the simulation, we assume that the standard deviation of time measurement noise is  $10^{-9}$  s (Considering the worst case of UWB).

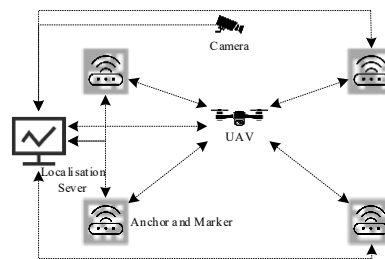


**Figure 3.** Localisation model

#### 4.1. Localisation system simulation

In Figure 4, the localisation system and the proposed VASTWTOF algorithm are simulated with UAV flying along a fixed path. In Figure 4(b), the green square represents the estimated position of anchor nodes, the blue line describes the true path of UAV and the red points depicts the estimated position calculated by the VASTWTOF. It can be observed that high accuracy localisation of UAV and anchor nodes was achieved through the VASTWTOF during the flight of UAV.

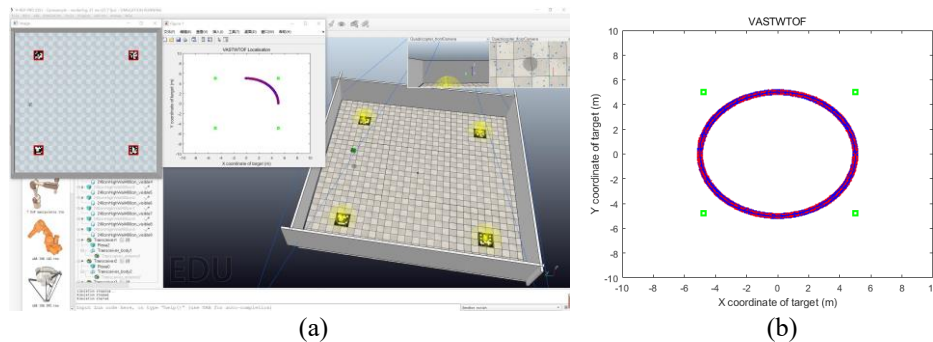


**Figure 4.** The simulation environment and localisation result for the VASTWTOF algorithm with UAV flying along a fixed path

#### 4.2. VASTWTOF algorithm simulation and discussion

In order to further discuss and analyse the performance of the VASTWTOF, much more simulations have been done from the different perspectives to demonstrate the effectiveness of the algorithm.

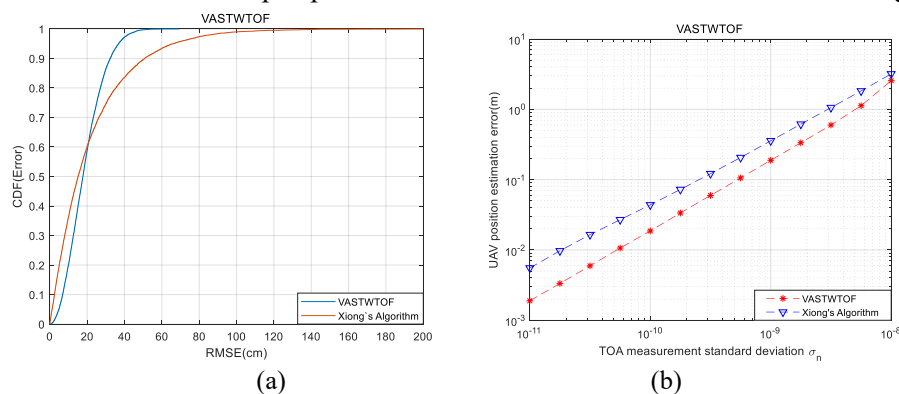


**Figure 5.** Error Cumulative Distribution Function (CDF) and UAV position estimate error comparison for the proposed VASTWTOF algorithm and the algorithm in [11]

As shown in Figure 5(a), the error CDF for the VASTWTOF and Xiong's algorithm in [11] are simulated. Where RMSE represents the root mean square error. From the error CDF, it is easy to observe that the median error (50 percentile) of the VASTWTOF is less than 20cm, and the 100-percentile error is about 50cm. For Xiong's algorithm, even the median error is superior to VASTWTOF, however, the VASTWTOF is much more stable and more accurate in most cases.

Finally, an 10000 times Monte Carlo simulation is carried out to test the localisation performance of the VASTWTOF under different TOA measurement noises. The VASTWTOF is also compared with Xiong's algorithm in [11]. Considering the propagation properties of the UWB based system, the measurement noise of TOA is around  $10^{-10} \sim 10^{-9}$  s. The simulation result in Figure 5(b) shows that there is always an obvious gap between the VASTWTOF and Xiong's algorithm when the measurement noise is around  $10^{-10} \sim 10^{-9}$  s. Moreover, the VASTWTOF has no requirements for any prior knowledge of anchor nodes.

## 5. Conclusion

A novel localisation algorithm (VASTWTOF) has been proposed in this paper for anchor self-localisation and precise UAV localisation in GPS-denied environment. This algorithm utilised the vision-based approach to aid the anchor self-localisation. Afterwards, the signal propagation delay between anchor nodes and UAV was leveraged to calculate the precise position information of UAV. This proposed algorithm possesses a great performance for localising UAV in different situations without the needs for any prior knowledge of anchor nodes. The simulation results illustrated the effectiveness of the proposed algorithm. In the future, further research will be done to expand the system to multiple UAVs in 3D scenarios.

## 6. Acknowledgments

This work is fully supported by the Research Excellence Award studentship from the University of Strathclyde and partly supported by "Low Cost Intelligent UAV Swarming Technology for Visual Inspection (LOCUST)" research project, funded by the UK Oil & Gas Technology Centre (Grant No. R180135-102-11603). The authors would also like to thank the OGTC robotics team at the University of Strathclyde for their kindly support.

## 7. References

- [1] Tripicchio, P., Satler, M., Unetti, M., & Avizzano, C. A. 2018. Confined spaces industrial inspection with micro aerial vehicles and laser range finder localization. *International Journal of Micro Air Vehicles*, **10(2)**, 207-224.
- [2] Yu, L., Yang, E., Ren, P., Luo, C., Dobie, G., Gu, D., & Yan, X. 2019. Inspection robots in oil and gas industry: a review of current solutions and future trends. In *2019 25<sup>th</sup> International Conference on Automation and Computing (ICAC)* (pp. 1-6). IEEE.
- [3] Bennett, T. R., Wu, J., Kehtarnavaz, N., & Jafari, R. 2016. Inertial measurement unit-based wearable computers for assisted living applications: *A signal processing perspective*. *IEEE Signal Processing Magazine*, **33(2)**, 28-35.
- [4] Ramirez, B., Chung, H., Derhamy, H., Eliasson, J., & Barca, J. C. 2016. Relative localization with computer vision and uwb range for flying robot formation control. In *2016 14th International Conference on Control, Automation, Robotics and Vision (ICARCV)* (pp. 1-6). IEEE.
- [5] Guo, K., Li, X., & Xie, L. 2019. Ultra-wideband and odometry-based cooperative relative localization with application to multi-UAV formation control. *IEEE transactions on cybernetics*, **50(6)**, 2590-2603.
- [6] Gao, F., Huang, T., Sun, J., Wang, J., Hussain, A., & Yang, E. 2019. A new algorithm for SAR image target recognition based on an improved deep convolutional neural network. *Cognitive Computation*, **11(6)**, 809-824.
- [7] Romero-Ramirez, F. J., Muñoz-Salinas, R., & Medina-Carnicer, R. 2018. Speeded up detection of squared fiducial markers. *Image and vision Computing*, **76**, 38-47.
- [8] OpenCV, Opencv.org, 2020. [Online]. Available: <https://opencv.org/>. [Accessed: 07- Oct-2020].
- [9] Sezgin, M., & Sankur, B. 2004. Survey over image thresholding techniques and quantitative performance evaluation. *Journal of Electronic imaging*, **13(1)**, 146-166.

- [10] Jiang, Y., & Leung, V. C. 2007. An asymmetric double sided two-way ranging for crystal offset. *In 2007 International Symposium on Signals, Systems and Electronics* (pp. 525-528). IEEE.
- [11] Xiong, H., Chen, Z., Yang, B., & Ni, R. 2015. TDOA localization algorithm with compensation of clock offset for wireless sensor networks. *China Communications*, **12(10)**, 193-201.